47th European Rotorcraft Forum
Glasgow, United Kingdom
7-10 September, 2021
Paper 15

PRACTICAL CONSIDERATIONS IN ROTOR DESIGN OPTIMISATION STUDIES

Thomas A. Fitzgibbon, Mark A. Woodgate and George N. Barakos
CFD Laboratory, School of Engineering, University of Glasgow, G12 8QQ, U.K.

Abstract

The present study demonstrates the application of an adjoint harmonic balance optimisation framework applied to the AH-64A blade. This framework allows for efficient optimisation of unsteady rotor flows whilst maintaining the fidelity of the Navier-Stokes equations. An analysis of the optimised rotor blade is presented, including the key design features that contribute to the performance benefits in each of the examined design conditions. The computational methodology and optimisation setup are analysed based on the impact on the final planform shape. The main areas of investigation include the interaction between the treatment of rotor solidity and trim state, and the employed parameterisation process as well as the impact of solution fidelity on the optimal shape. The employed methodology leads to significant performance benefits, however, the present analysis shows that there is potential for further improvements.

1 INTRODUCTION

Rotor design is an important topic within the rotorcraft community despite the maturity of the dominant helicopter configuration - main rotor/tail rotor. Improved rotor designs can lead to reduced fuel consumption, expanded flight envelopes as well as reduced noise/vibration. The emergence of more advanced planform shapes such as the BERP design [1], Blue-Edge blade [2] or Advanced Chinook Rotor Blade (ACRB) [3] show us that rotor design is still progressing. A number of studies have emerged in the literature concerning rotor design optimisation [4–9] using both gradient-based and non-gradient based optimisation methods as well as aerodynamic solutions of different levels of fidelity. Previous studies have also shown that high-fidelity solutions need to be included within the optimisation process, especially when capturing the aerodynamics of advanced planform shapes [4, 10, 11]. The main difficulty in rotor blade optimisation is the need for optimisation of unsteady flows leading to extremely high computational costs. Non-gradient optimisation methods are typically limited by the number of flowfield evaluations and/or the number of required design parameters due to the need for expensive time-accurate CFD simulations. Similarly, gradient-based methods based on time-accurate adjoint frameworks [6, 12] can also be considered as computationally expensive due to the requirement to store the entire flow solution history for back propagation as required for the adjoint solution. Time-spectral methods offer a significant speed-up compared to time-accurate simulations [13] as they treat the solution as a large steady problem with an unsteady source term by

assuming periodicity in time. The nature of frequency domain methods also make them attractive for adjoint optimisation studies, as the steady adjoint solver (with certain modifications) can be used. The only application of a time-spectral adjoint method to rotorcraft flows was demonstrated by Choi et al. [7] in a optimisation study of the UH-60A rotor blade. The optimisation was performed on coarse matched grids for inviscid flows using a single blade assumption, thereby neglecting unsteady wake effects.

The present study builds on previous optimisation results [14], which demonstrated the use of an optimisation framework based on a fully-turbulent overset adjoint harmonic balance method applied to the AH-64A rotor blade. The results are analysed in the context of discussing some of the practical considerations in rotor design, including the interaction between rotor solidity, trim and the blade surface parameterisation and the impact of solution fidelity on the final shape.

2 NUMERICAL METHODOLOGY

The employed optimisation framework is based on the adjoint-harmonic balance method which has been implemented within the HMB3 solver of Glasgow University [15, 16]. The harmonic balance method allows us the treat the flow as a large steady solution (with an additional source term which accounts for the flow unsteadiness), leading to a significant cost reduction compared with a time-dependent adjoint formulation (in both time and disk space/memory). The harmonic balance implementation is described in [13] with an extension to overset grids presented in [17]. The adjoint formulation computes the gradients of a single objective function with respect to all the design variables at the cost of a base flow solution. This is significantly cheaper than non-gradient methods which require an order of N^2-N^3 (number of design variables) simulations to obtain an optimal solution. The full implementation of the adjoint method is given by Biava et al. [18] with the present work developing the method to include shape design sensitivities. The adjoint harmonic balance method allows for optimisation of unsteady rotor flows with modest computational resources.

The complete optimisation framework is described as follows. Firstly, the baseline flow solution is computed using the steady state solver or the harmonic balance method. The baseline objective function and constraints are then evaluated from the base flow solution. The adjoint problem is then solved, and the design sensitivities are computed using the adjoint method. The cost functional, the constraints and their gradients are fed to the gradient based optimiser, to obtain a new design variable vector. In our tool chain, the Least-Square Sequential Quadratic Programming (SLSQP) algorithm [19] is used. Based on the new vector of design variables the surface to be optimised is deformed based on an external parameterisation tool (details in next subsection). The parameterisation outputs the coordinates of the new surface as well as the surface sensitivities which are used in the adjoint method. Finally, a mesh deformation algorithm based on Inverse-Distance Weighting is employed to update the volume mesh. The optimisation workflow loop is continued until a stopping criterion is reached, which is in this case is either an update tolerance on the objective function or the design variables.

2.1 Blade surface parameterisation method

A deformative blade surface parameterisation method is used, where the movements of the blade surface mesh points are described analytically, and the volume mesh is updated using an IDW method. The twist law is parameterised using a Bernstein polynomial function with seven coefficients. The chord is altered at four radial stations of r/R = 0.5, 0.75, 0.943 and 1.0; whereas the sweep and anhedral angles are changed at the three outboard radial stations of r/R = 0.75, 0.943 and 1.0. Linear distributions are imposed inboard of 0.943, with parabolic distributions of the blade chord, sweep and anhedral angles across the blade tip region from 0.943 R to 1.0 R. This leads to a total of 17 design parameters. The blade planform parameterisation is shown in Figure 1. As a deformative method is used, the parameters are applied as a change to the baseline surface mesh. Here, the blade tip sweep is removed before applying the new set of parameters, hence a rectangular blade with -9 degrees linear blade twist is used (closely resembling the AH-64A blade). The design parameter boundaries are shown in Table 1.

3 BLADE GEOMETRY AND COMPUTATIONAL SETUP

To demonstrate the developed optimisation framework, the AH-64A rotor blade was selected. This rotor blade is well-documented in the open-literature [20, 21] to perform validation studies and then optimise its planform. The AH-64A blade was also chosen as it operates at high load. The full scale rotor blade planform scaled to a unit chord of 1.0 is shown in Figure 2, with the blade having a dimensional radius of 288 inches and a chord of 21 inches. The AH-64A rotor blade has a swept tip, a linear blade twist of nominally -9 degrees and an aspect ratio of 13.714. The blade is composed of two aerofoil sections, the HH-02 section up to 0.943R and the NACA64A006 section at the tip of the blade. Details of the blade geometric properties and their uncertainties can be found in [17].

All simulations were performed for isolated and rigid rotors to reduce the computational costs. In hover, the steady state formulation was used. Only a quarter of the computational domain was meshed, assuming periodic conditions for the flow field in the azimuthal direction. In forward flight, the full rotor disk was modelled for both time-marching and harmonic balance simulations as the flow is highly unsteady. A matrix trimming routine was used to achieve the set target thrust coefficient whilst minimizing the pitching and rolling moments [16]. Multi-block structured meshes are generated for the AH-64A blade using ICEM-HEXA and the overset grid technique. In hover, as only one blade is modelled, 10.7 million cells were used to resolve the domain, whereas 36.1 million cells were used in forward flight for the full rotor disk. The optimisation was performed on a coarser grid of 13.1 million cells to reduce the memory demands of the simulation for the adjoint-harmonic balance method. All computations were performed for a blade tip Mach number of 0.65 and Reynolds number of 7.98×10^6. Performance predictions for the AH-64A blade have been computed based on experimental data from [20], and compared with HMB3 results in [15]. Validation studies have also been performed for the harmonic balance solver in previous work [17].

4 RESULTS AND DISCUSSION

Firstly, the resulting blade design from the optimisation study is presented. Following this various aspects of the design are analysed in terms of practical design considerations.

4.1 Optimisation Results

The optimisation results were presented in detail in previous works [14, 15]. Here, we present the final design obtained through a sequential hover forward flight optimisation study before conducting further analysis of the employed methodology and the blade design. The optimisation was performed using the adjoint harmonic balance method, with a time-accurate simulation performed to verify the optimisation results. The final blade design is shown in Figures 3-4. The optimiser leads to a final design with increased blade twist compared to the baseline AH-64A blade. The blade twist is a key hover performance driver leading to an offloaded blade tip and a shifting of the load inboard. However, in this case, increased blade twist was also found to be beneficial in forward flight, with a slightly increased tip loading preferred, compared to the hover result. The chord distribution leads to a planform with maximum chord inboard, with a significantly reduced tip area, leading to a reduction in both profile and induced power through a more favourable blade loading. The forward flight optimised blade also has a forward-backward sweep distribution, mainly aimed at reducing compressibility effects. The dihedral-anhedral distribution was carried over from the hover optimisation and was not changed during the forward flight optimisation. In hover, this design feature offloads the blade tip and leads to a weaker blade tip vortex as well as minimized blade tip vortex interaction. The performance benefits of the final design are presented in Table 2.

The hover performance is significantly improved compared to the baseline blade, as a benefit of 6.1 counts in FoM is obtained at $C_T = 0.0093$, along with a 6.5% improvement in forward flight. The final design has an offloaded blade tip compared to the baseline AH-64A blade, through the introduction of a non-linear twist distribution, along with a forward-backward sweep distribution leading to a further reduction in the pressure torque term. The viscous torque term is slightly increased due to dihedral-anhedral distribution leading to a

more non-planar planform along with the higher inboard chord. The optimised blade also leads to a trim state with a higher collective angle (+0.9 deg) and lower longitudinal cyclic (-1.1 deg) when compared to the baseline AH-64A blade, which leads to a more uniform rotor disk blade incidence distribution, thereby contributing to the improved performance.

4.2 Impact of Solution Fidelity

Firstly, the impact of solution fidelity is assessed to determine what effect the computational method has on the optimal shape. For this purpose, the rotor disk loads are compared between the time-marching simulation on the finer grid (36.1M cells) and the two harmonic balance mode solutions on a coarser grid (13.1M) used during the optimisation study. The rotor disk loads, shown in Figure 5, are scaled by a reference chord equal to the chord of the first aerodynamic section. The M^2C_l and M^2C_d represent force in the normal and tangential directions (non-radial) to the rotor disk plane representing the local lift and drag values uncorrected for downwash effects (hence, thrust and torque/(local radius)).

Based on the rotor disk loads, it can be seen that the loads for the baseline AH-64A blade are captured well. The greatest differences can be seen in the capturing of the negative pitching moment on the retreating side due to dynamic stall. This is a high frequency phenomenon which is likely to require a higher number of harmonic balance modes for a more accurate representation. Therefore, it can be stated that the optimiser did not target the retreating side aerodynamics to improve the overall rotor performance. Similar observations can be made for the optimised planform, as the general loads trends are well predicted by the harmonic balance method. The optimised rotor disk loads indicate the presence of higher-harmonic content in the lift force loading as the blade passes from the advancing side to the front of the rotor disk, which is not captured by the harmonic balance solutions. This is also a higher frequency phenomenon which could be captured more accurately with a higher number of harmonic balance modes. Based on the current observations, the optimiser targeted improvements in the loading of lower frequencies due to the employed time discretisation used in the harmonic balance method. Higher frequency phenomena may need to be captured more accurately by using a higher number of harmonic balance modes, should noise/vibration objectives be included in future work. It must, however, be noted that lower fidelity models (comprehensive rotor codes) would also fail to accurately capture these effects, and might also lead to worse predictions of the lower frequency loading, for which the two mode harmonic balance solutions show very good predictions. The harmonic balance method also generally predicted a slightly lower power improvement for the optimised blade when compared with the baseline AH-64A blade (-5.1% compared to -6.5%) mainly due to increased levels of turbulent eddy viscosity ratio in the rotor wake. The grid resolution did not seem to greatly affect the optimisation result as the general loading is well captured.

4.3 Impact of Parameterisation, Treatment of Solidity and Trim

The impact of the parameterisation, treatment of solidity and trim state is analysed next. One of the key outcomes of the optimisation process is the significantly increased inboard planform area and hence increased geometric and thrust-weighted solidity. However, this is not an aerodynamic performance effect, but rather the impact of the trim treatment. Even though the solidity was not constrained, it is claimed that this aspect did not impact the final planform shape. A higher solidity (geometric) rotor will lead to a shift in the maximum figure of merit value to higher thrust coefficients by delaying the onset of stall. For this reason, the solidity (in many cases thrust-weighted) of a rotor is constrained in many hover optimisation studies [5,22,23], when the objective is to maximize the figure of merit. This can be avoided by reformulating the objective as a power minimization problem at constant thrust, which was done in the current optimisation study. The power required at a specific weight is more important in real-life rotor design than the figure of merit value. Furthermore, as postulated by Perry [24] and confirmed in previous work [25], the definition of thrust-weighted solidity is misleading and will promote planforms with lower area at the blade tip. The main reason for the use of thrust-weighted solidity is to account for the additional blade weight of a blade with additional area near the blade tip, as seen for example in BERP-like designs. However, as stated by Perry [24] the weight increase is of second order

due to the outer structure of the blade only being a light fairing. In the present study, the planform area increase is further inboard and is likely to impact the blade weight, however, the blade mass should directly be used as a constraint in the optimisation formulation.

The main reason for the increase in planform area for the optimised blade is the blade surface parameterisation and treatment of trim. This is due to the imposed thrust constraint at a fixed collective. The interaction between the optimum planform shape and the collective angle should be examined further, as part of future work. In hover, higher blade twist is generally favourable for improved hover performance, however, more highly twisted blades, require a higher collective angle to achieve the same thrust coefficient. In this case, the main design feature that recovers the thrust is the high inboard chord, which may be reduced should the collective angle be included within the design parameters. A similar result is obtained in forward flight as the control angles are not directly included as design variables. Shape updates in this case also cause an imbalance in roll/pitch which require a special treatment to ensure that each objective function evaluation is performed for a trimmed rotor. The process included a partial re-trim for moments and a full optimisation restart with a full re-trim every few optimiser iterations. This procedure was required as the trim state is not directly included within the optimisation loop. Similarly, as in hover, the final planform shape may be influenced by the non-inclusion of trim variables within the optimisation process and lack of any constraints on the pitching and rolling moments. Therefore, it can not be stated with full confidence whether the optimiser is driving the design to a better aerodynamic shape or a design that generates rolling and pitching moments that reduce the rotor power. In particular, it was found that designs which generated a positive integrated pitching moment and a rolling moment from the advancing side to the retreating side were beneficial to the rotor power. This is one of the difficulties associated with forward flight rotor optimisation, as the rotor power is actually more sensitive to the rotor trim state rather than the rotor shape. A higher blade twist leads to the production of an unfavourable rolling moment on the rotor power, but is more beneficial aerodynamically, by offloading the blade tip. After re-trimming to the same thrust of the new design and minimizing the pitching and rolling moments, the power goes down further. This is mainly due to a lower longitudinal cyclic requirement for a highly twisted blade. The only features that increase the thrust of the blade are higher blade planform area or by modifying the angle of incidence along the span of the blade (blade twist). The reduced planform area and negative incidence at the blade tip led to a greater reduction in power than reduction in thrust. Hence, increasing the planform area inboard was seen as the main feature that recovers this thrust loss. However, the high planform area inboard may not be optimal, and should trim variables be included within the optimisation process, a better design may be found at a different trim state (for example lower blade area at a higher collective).

The impact of the employed parameterisation also has a certain impact on the final design. Firstly, the radial stations and distributions between them of the chord, sweep and anhedral laws were prescribed and hence may not be optimal. Another key feature of the blade surface parameterisation can be demonstrated by examining the advancing side surface pressure distribution shown in Fig 6. The optimised blade shows a significantly weaker shock compared to the baseline AH-64A blade, however, this shock is not completely removed showing the potential for further improvements. The shock is moved further inboard and moved into the region of the HH02 aerofoil. The manner in which the optimisation was set up, however, maintained the aerofoil shape with chord changes, hence the thickness/chord ratio was maintained. The separation of chord and aerofoil thickness parameters may have increased the chord in this region, leading to a reduced thickness to chord ratio and therefore, potentially removing the shock completely. In this case, as the thickness to chord ratio was held constant, the optimiser reduced to local chord to reduce viscous effects and further offload the blade tip. Therefore, the reduction in blade tip area was found to be more beneficial to the rotor power than complete removal of the advancing blade shock. The forward sweep leads to a weakening of this shock, whereas the actual blade tip carries very little loading. In the future, the aerofoil shape could also be optimised to improve the advancing blade aerodynamics.

4.4 Impact of Aeroelasticity

The non-inclusion of aeroelastic effects is likely to also have an impact on the resulting planform shape. The inclusion of aeroelastic effects would capture the effects of down flap on the advancing side and up flap at the front and back of the rotor disk which were not included within the rigid blade simulations (as they were trimmed to zero flapping). However, the main effect that is likely to affect performance is the elastic torsion. In hover, the elastic torsion increases the blade twist for blades with a swept back blade tip, hence could potentially lead to increased performance, especially at conditions away from stall. In forward flight, blade untwisting on the advancing side is desirable along with increased blade twist on the retreating side. The optimised blade must also be assessed in terms of safety and control loads. The forward-backward swept planform is likely due to produce higher lag bending moments due to the offsets from the elastic axis. Similarly, the non-planar planform shape is likely to introduce increased flap bending moments.

5 CONCLUSIONS AND FUTURE WORK

This paper has demonstrated the application of a high fidelity optimisation framework to the redesign of the AH-64A rotor blade in hover and forward flight. The study showed that significant benefits are achievable by coupling high-fidelity CFD with optimisation methods. The harmonic balance-adjoint optimisation method offers an efficient way to obtain the CFD solution and design variable gradients for unsteady optimisation problems whilst maintaining the fidelity of the Navier-Stokes equations. The key drivers of an improved rotor design in hover and forward flight are an offloaded blade tip through an increased blade twist and dihedral-anhedral distribution which lead to a more optimal trim state in forward flight, weaker blade tip vortices and a more favourable spanwise loading distribution.

The paper also elaborates on the impact of various features of the computational method on the final planform shape. Based on this discussion, suggestions are put forward for future work. The trim state should be optimised together with the planform shape with additional constraints on the pitching and rolling moments, to fully capture the interaction between planform shape, solidity and the rotor control angles. A higher number of harmonic balance modes should be included within the CFD solution, to capture and optimise higher frequency content phenomena. A more elaborate blade surface parameterisation should also be included to enable the exploration of a wider design space. The inclusion of aeroelastic effects should also be a subject of future work, ensuring that realistic blade designs are obtained that can be used in practice.

6 Acknowledgments

This work is funded by DSTL (Defence Science and Technology Laboratory). A part of the technical work has been completed under the collaboration project, TTCP AER CP13.A1, Next Generation Rotor Blade Design. This work used the Cirrus UK National Tier-2 HPC Service at EPCC (http://www.cirrus.ac.uk). This work used the ARCHER UK National Supercomputing Service (http://www.archer.ac.uk).

7 REFERENCES

References

[1] Perry, F., “Aerodynamics of the World Speed Record,” *43rd Annual Forum of the American Helicopter Society*, St. Louis, Missouri, 1987.

[2] Rauch, P., Gervais, M., Cranga, P., Baud, A., Hirsch, J., Walter, A., and Beaumier, P., “Blue Edge (TM): The Design, Development and Testing of a New Blade Concept,” *American Helicopter Society 67th Annual Forum*, Virginia Beach, Virginia, 2011.

[3] Boeing, “New Chinook Composite Blades Proven,” `http://www.boeing.com/features/2017/01/chinook-blades-01-17.page`, 2017, [Online; accessed 22-March-2018].

[4] Wilke, G., “Variable Fidelity Optimization of Required Power of Rotor Blades: Investigation of Aerodynamic Models and their Application,” *38th European Rotorcraft Forum*, Amsterdam, The Netherlands, 2012.

[5] Imiela, M., "High-fidelity optimization framework for helicopter rotors," *Journal of Aerospace Science and Technology*, Vol. 23, No. 1, 2012, pp. 2–16, DOI: 10.1016/j.ast.2011.12.011.

[6] Wang, L., Diskin, B., Biedron, R., Nielsen, E., and Bachau, O., "High-Fidelity Multidisciplinary Sensitivity Analysis and Design Optimization for Rotorcraft Applications," *AIAA Journal*, Vol. 57, No. 8, 2019, pp. 1–15, DOI: 10.2514/1.J056587.

[7] Choi, S., Lee, K., Potsdam, M., and Alonso, J., "Helicopter Rotor Design Using a Time-Spectral and Adjoint-Based Method," *Journal of Aircraft*, Vol. 51, No. 2, 2014, pp. 412–423, DOI: 10.2514/1.C031975.

[8] Leusink, D., Alfano, D., Cinnella, P., and Robinet, J., "Aerodynamic rotor blade optimization at Eurocopter - a new way of industrial rotor blade design," *51st AIAA Aerospace Sciences Meeting*, 2013.

[9] Massaro, A., D'Andrea, A., and Benini, E., "Multiobjective-Multipoint Rotor Blade Optimization in Forward Flight Conditions Using Surrogate-Assisted Memetic Algorithms," *37th European Rotorcraft Forum*, Cascina Costa, Italy, 2011.

[10] Bailly, J. and Bailly, D., "Multifidelity Aerodynamic Optimization of a Helicopter Rotor Blade," *AIAA Journal*, Vol. 57, No. 8, 2019, pp. 3132–3144, DOI: 10.2514/1.J056513.

[11] Desvigne, D., Coisnon, R., Michel, B., Thomas, A., Pinacho, J., and Roca-Leon, E., "Multi-Objective Industrial Optimization of High-Speed Helicopter Main Rotor Blades with Dynamically-Adpated Structural Properties," *45th European Rotorcraft Forum*, 2019.

[12] Fabiano, E. and Mavriplis, D., "Adjoint-based Aeroacoustic Design-Optimization of Flexible Rotors in Forward Flight," *American Helicopter Society 72nd Annual Forum*, 2016.

[13] Woodgate, M. and Barakos, G., "Implicit Computational Fluid Dynamics Methods for Fast Analysis of Rotor Flows," *AIAA Journal*, Vol. 50, No. 6, 2012, pp. 1217–1244.

[14] Fitzgibbon, T., Barakos, G., and Woodgate, M., "Optimisation of the AH-64A Blade Planform Based on High-Fidelity CFD Methods," *Vertical Flight Society 77th Annual Forum and Technology Display*, Virtual.

[15] Fitzgibbon, T., *Advanced Rotor Blade Design based on High-Fidelity Computational Fluid Dynamics*, Ph.D. thesis, University of Glasgow, 2021.

[16] Steijl, R., Barakos, G. N., and Badcock, K., "A framework for CFD analysis of helicopter rotors in hover and forward flight," *International Journal for Numerical Methods in Fluids*, Vol. 51, No. 8, 2006, pp. 819–847, DOI: 10.1002/d.1086.

[17] Fitzgibbon, T., Woodgate, M., and Barakos, G., "Assessment of the Harmonic Balance Method for Rotor Blade Performance Predictions," *45th European Rotorcraft Forum*, 2019.

[18] Biava, M., Woodgate, M., and Barakos, G., "Fully Implicit Discrete-Adjoint Methods for Rotorcraft Applications," *AIAA Journal*, Vol. 54, No. 2, 2016, pp. 735–748.

[19] Kraft, D., "Algorithm 733: TOMP-Fortran Modules for Optimal Control Calculations," *ACM Transactions on Mathematical Software*, Vol. 20, No. 3, 1994, pp. 262–281.

[20] JanakiRam, R., Smith, R., Charles, B., and Hassan, A., "Aerodynamic Design of a New Affordable Main Rotor for the Apache Helicopter," *American Helicopter Society 59th Annual Forum*, 2003.

[21] Berry, J., "Helicopter Blade Dynamic Loads Measured During Performance Testing of Two Scaled Rotors," Tech. rep., National Aeronautics and Space Administration, 1987, NASA-TM-89053.

[22] Dumont, A., Le Pape, A., Peter, J., and Huberson, S., "Aerodynamic Shape Optimization of Hovering Rotors Using a Discrete Adjoint of the Reynolds-Averaged Navier-Stokes Equations," *Journal of the American Helicopter Society*, Vol. 56, No. 3, 2011, pp. 1–11, DOI: 10.4050/JAHS.56.032002.

[23] Leon, E., Le Pape, A., Desideri, J., Alfano, D., and Costes, M., "Concurrent Aerodynamic

Optimization of Rotor Blades Using a Nash Game Method," *Journal of the American Helicopter Society*, Vol. 61, No. 2, 2016, pp. 1–13, DOI: 10.4050/JAHS.61.022009.

[24] Perry, F., "Technical Note: The Contribution of Planform Area to the Performance of the BERP Rotor (Reply to Kenneth B. Amer)," *Journal of American Helicopter Society*, Vol. 34, No. 1, 1989, pp. 64–65, DOI: 10.4050/JAHS.34.64.

[25] Fitzgibbon, T., Woodgate, M., and Barakos, G., "Assessment of current rotor design comparison practices based on high-fidelity CFD methods," *The Aeronautical Journal*, Vol. 124, No. 1275, 2020, pp. 731766.

8 TABLES AND FIGURES

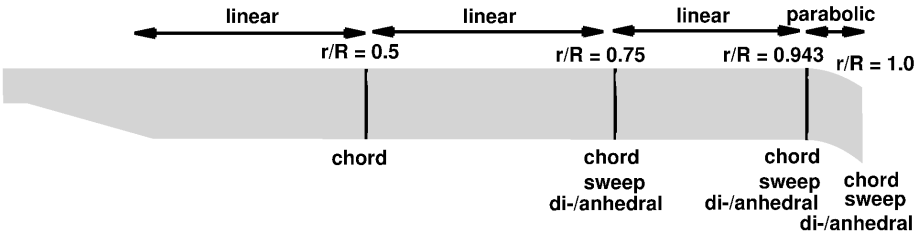

Figure 1: Blade surface parameterisation shown based on the AH-64A blade used within optimisation study.

Table 1: Design parameter upper and lower boundaries used during the AH-64A optimisation study.

Design Parameter	Boundary values
TWIST1 - TWIST7	± 5 deg
CHORD at r/R = 0.5	[0.8c,1.4c]
CHORD at r/R = 0.75	[0.8c,1.4c]
CHORD at r/R = 0.943	[0.8c,1.4c]
CHORD at r/R = 1.0	[0.3c,1.5c]
SWEEP at r/R = 0.75	[-0.3c,0.4c]
SWEEP at r/R = 0.943	[-0.3c,0.4c]
SWEEP at r/R = 1.0	[-0.7c,0.4c]
ANHEDRAL at r/R = 0.75	[-0.1c,0.25c]
ANHEDRAL at r/R = 0.943	[-0.1c,0.25c]
ANHEDRAL at r/R = 1.0	[-0.25c,0.1c]

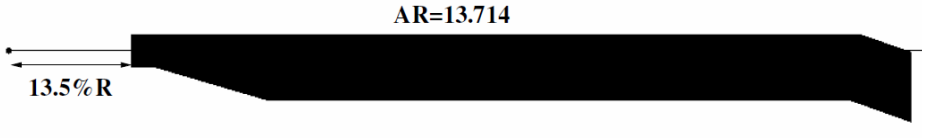

Figure 2: Planform of the AH-64A blade scaled to a unit chord.

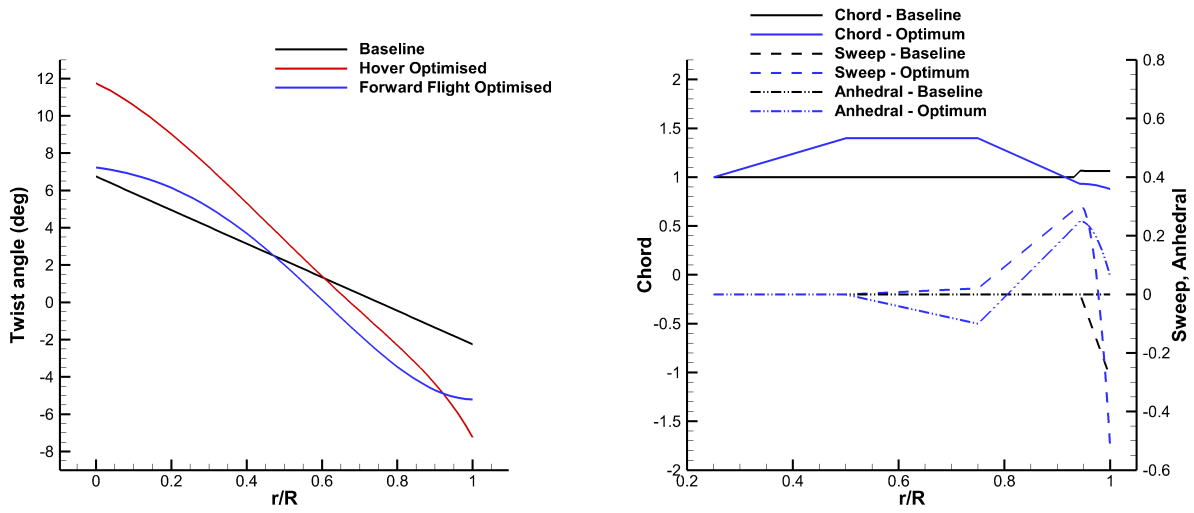

(a) Twist law

(b) Chord, Sweep and Anhedral laws

Figure 3: Comparison of baseline AH-64A and forward flight optimised geometric laws. Chord, Sweep and Anhedral values given based on a unit chord length (chord of first aerodynamic section).

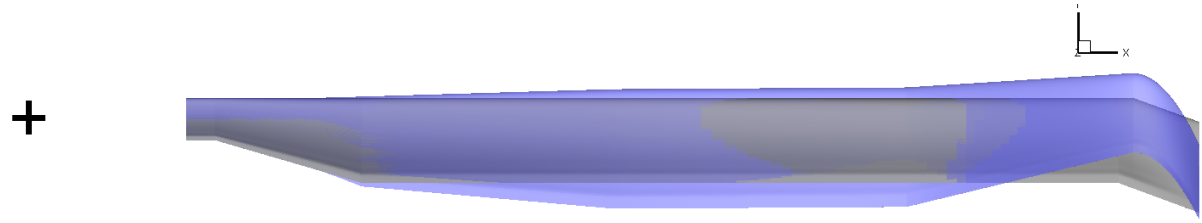

(a) Top view

(b) Side view

Figure 4: Comparison between the baseline (grey) and forward flight optimised (blue) planform shapes for the AH-64A rotor blade in forward flight at $C_T = 0.00903$, $\mu = 0.3$.

Table 2: Comparison of the integrated loads between the baseline and optimised AH-64A planforms.

Planform	**Baseline AH-64A**	**Optimised AH-64A**
Hover Figure of Merit ($C_T = 0.0093$)	0.696	0.757 (+6.1 counts)
FF, C_Q ($C_T = 0.00903, \mu = 0.3$)	6.984×10^{-4} (-)	6.529×10^{-4} (-6.51%)
C_{Qp}	6.097×10^{-4}	5.462×10^{-4}
C_{Qv}	8.870×10^{-5}	1.066×10^{-4}

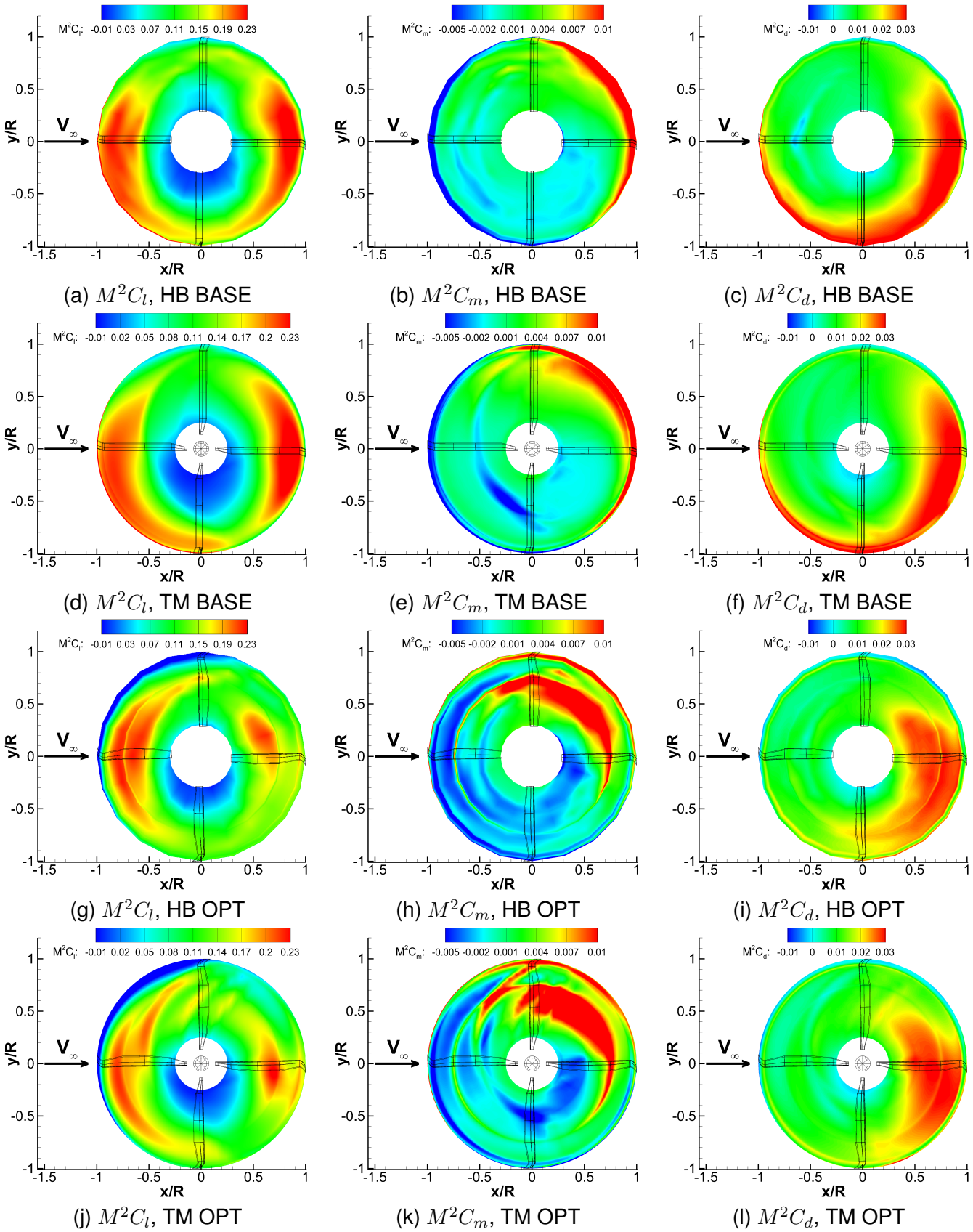

(a) M^2C_l, HB BASE (b) M^2C_m, HB BASE (c) M^2C_d, HB BASE

(d) M^2C_l, TM BASE (e) M^2C_m, TM BASE (f) M^2C_d, TM BASE

(g) M^2C_l, HB OPT (h) M^2C_m, HB OPT (i) M^2C_d, HB OPT

(j) M^2C_l, TM OPT (k) M^2C_m, TM OPT (l) M^2C_d, TM OPT

Figure 5: Comparison of the rotor disk loads for the baseline (BASE) parameterised and optimised (OPT) AH-64A rotor blades in forward flight at $C_T = 0.00903$, $\mu = 0.3$ based on 2 mode harmonic balance (HB) and time-marching (TM) calculations.

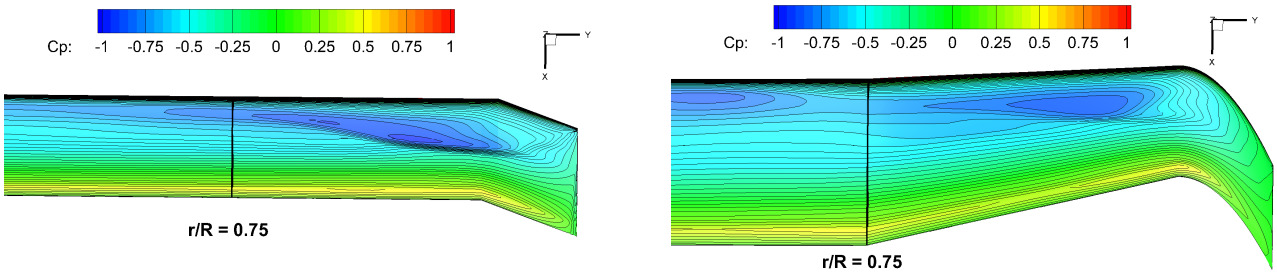

(a) Baseline (b) Optimised

Figure 6: Comparison between the baseline and optimised advancing side surface pressure distributions at $C_T = 0.00903, \mu = 0.3$.